Title: **Effects of Soot Morphology and Chemistry on Particle Hygroscopic and Optical Properties. FINAL PROGRESS REPORT December 10, 2011**

Project ID: 0011068
Program Manager: Ashley D. Williamson, Phone: 301-903-3120 Division: SC-23.1
PI: Paul Davidovits
Award Register#: ER63995 0011068
Award Period: 01/01/2005 to 12/31/2011; the final year was a no-cost extension.

1. Introduction.

Soot particles are generated by incomplete combustion of fossil and biomass fuels. Through direct effects clear air aerosols containing black carbon (BC) such as soot aerosols, absorb incoming light heating the atmosphere, while most other aerosols scatter light and produce cooling. Even though BC represents only 1-2% of the total annual emissions of particulate mass to the atmosphere, it has been estimated that the direct radiative effect of BC is the second-most important contributor to global warming after absorption by CO_2. Ongoing studies continue to underscore the climate forcing importance of black carbon. However, estimates of the radiative effects of black carbon on climate remain highly uncertain due to the complexity of particles containing black carbon.

Quantitative measurement of BC is challenging because BC often occurs in highly non-spherical soot particles of complex morphology. Freshly emitted soot particles are typically fractal hydrophobic aggregates. The aggregates consist of black carbon spherules with diameters typically in the range of about 15-40 nm, and they are usually coated by adsorbed polyaromatic hydrocarbons (PAHs) produced during combustion. Diesel-generated soot particles are often emitted with an organic coating composed primarily of lubricating oil and unburned fuel, as well as well as PAH compounds. Sulfuric acid has also been detected in diesel and aircraft-emitted soot particles. In the course of aging, these particle coatings may be substantially altered by chemical reactions and/or the deposition of other materials. Such processes transform the optical and CCN properties of the soot aerosols in ways that are not yet well understood.

Our work over the past seven years consisted of laboratory research, instrument development and characterization, and field studies with the central focus of improving our understanding of the black carbon aerosol climate impacts. During the sixth year as well as during this seventh year (no-cost extension period) of our grant, we extended our studies to perform experiments on the controlled production and characterization of secondary organic aerosol.

2. Laboratory Research

2.1 Source for Generation of Well Characterized Soot Particles. An essential part of performing reproducible reliable experiments with soot particle is the availability of a well-characterized, stable source of soot particles. Such a source has been developed in our laboratory and is shown in Figure 1. Soot particles are generated by the combustion of a mixture of fuel (ethylene in the current studies) and oxygen in a commercially available McKenna burner. The particles are sampled through an inlet consisting of two concentric stainless steel tubes. Particles travel up the inner tube while a carrier gas (N_2) flow passes down the outer tube and then back up the inner tube. The gas flow around the lip of the inner tube prevents soot

buildup in this region and is used to control the total number concentration of sampled particles (via dilution).

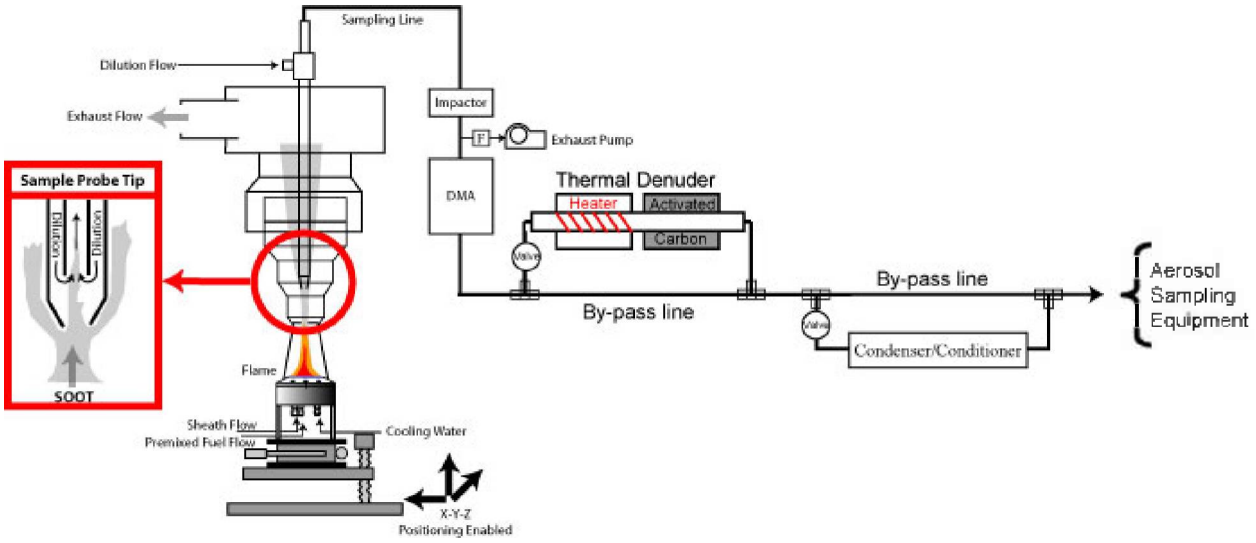

Figure 1. Boston College laboratory flame generation and conditioning apparatus.

The base of the burner is mounted on an x-y-z translation stage and the combined soot generation-sampling apparatus is secured on a stainless steal frame attached to an optical table. This arrangement provides a stable reproducible alignment of the sampling inlet with the soot source. The apparatus has been continually improved and can now provide monodisperse, size selected soot particles in the range 30 to 500 nm and over a fuel-to-air equivalence ratio from 1.8 to 6.0 (generating soot particles with primary spherules that vary from 15-45 nm in diameter and with varying organic coatings). SEM images of soot as a function of equivalence ratio are shown in Figure 2.

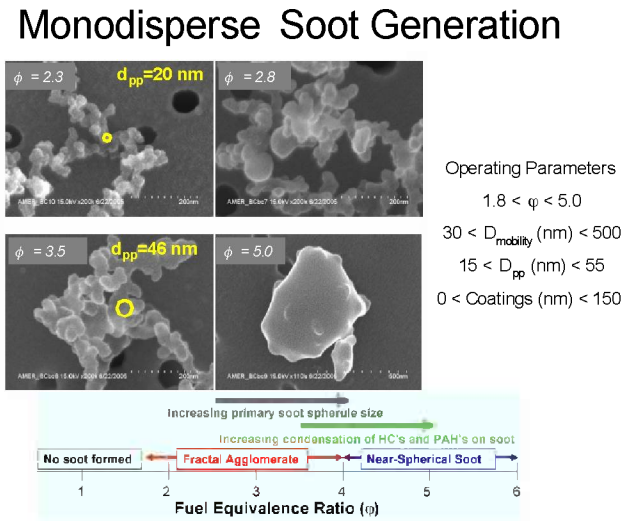

Figure 2. SEM images of laboratory generated soot particles as a function of fuel-to-air equivalence ratio.

The particles are well characterized with respect to mobility and aerodynamic diameters, composition and fractal dimension. The particles can be coated with layers of organics, ammonium salts and water in a controlled way. The experimental apparatus is equipped with a denuder to remove the non-refractory components of the soot particles, if so desired. The fuel-to-air ratio, particle concentration, relative humidity, flow rates, etc. are all controlled and measured. The details of the apparatus and methods of particle characterization are described in *Jayne et al.* 2000, *Slowik et al.* 2004, *DeCarlo et al.* 2004, *Slowik et al.* 2007a, Slowik et al. 2007b, *Canagaratna et al.*, 2007, *Hings et al.* 2008, *Charabarty et al.*, 2007, 2008, 2009

2.2 Improvement of the Soot-generating Apparatus. During the sixth year of our grant the soot generation apparatus was redesigned to improve stability and reproducibility of the black carbon particle produced. An important modification was the introduction of Venturi-effect valves to provide a constant flow into the soot-sampling tip. As is discussed below the resulting poly-disperse distribution provides a stable mono-disperse population of soot particles.

The sampling system now includes a stagnation point produce by a compressed fiberglass disk (6 cm diameter). This configuration interrupts the conical flame shape causing the gas to travel around the disk. The flow is diluted by the sheath gas resulting in the formation of smaller particles in the sampling region. This configuration provides more stable number concentration in the sampled flow and also a more consistent poly-disperse size distribution. The standard deviation of the number concentration improved from +/-30percent to +/- 15 percent. With the new system it is possible to obtain a more stable polydisperse size distribution and consequently also a more stable monodisperse distribution. The temperature of the flame base through which the premix flows was also increased to provide greater homogeneity in the premix as it goes through the porous copper frit.

These improvements have and will aid our continuing studies to characterize optical, physical, and chemical properties of soot particles.

2.3 Effect of Coatings on Particle Properties. Field studies have shown that soot particles in the atmosphere become coated often rapidly with organic and/or inorganic compounds. The organic coatings are usually generated via photo-oxidation of gas phase organics followed by gas-to-particle condensation. Inorganic coatings are usually nitrate or sulfate products of gas phase ammonia reactions with acids. It is important to understand the effect of such coatings on particle morphology, CCN activity, and optical properties.

2.3.1 CCN Activation Experiments with Adipic Acid: Effect of Particle Phase and Adipic Acid Coatings on Soluble and Insoluble Particles.

Slightly soluble atmospherically relevant organic compounds may influence particle CCN activity and therefore cloud formation. Adipic acid is a frequently employed surrogate for such slightly soluble organic materials. The 11 published experimental studies on CCN activity of adipic acid particles are not consistent with each other nor do they, in most cases, agree with the Köhler theory. The CCN activity of adipic acid aerosol particles was studied over a significantly wider range of conditions than in any previous single study. The experiments suggest that the scatter in the previously published CCN measurements is most likely due to the difficulty of producing uncontaminated adipic acid particles by atomization of solutions and possibly also due to uncertainties in the calibration of the instruments. The CCN activation of the small (d_m < 150 nm) initially dry particles is subject to a deliquescence barrier, while for the larger particles the activation follows the Köhler curve. Wet adipic acid particles follow the

Köhler curve over the full range of particle diameters studied. When a water-soluble core is coated by adipic acid, the CCN-hindering effect of particle phase is eliminated. Figure 3 shows the effects of phase on the CCN activity of adipic acid particles. This work is described in detail in *Hings et al. 2008*.

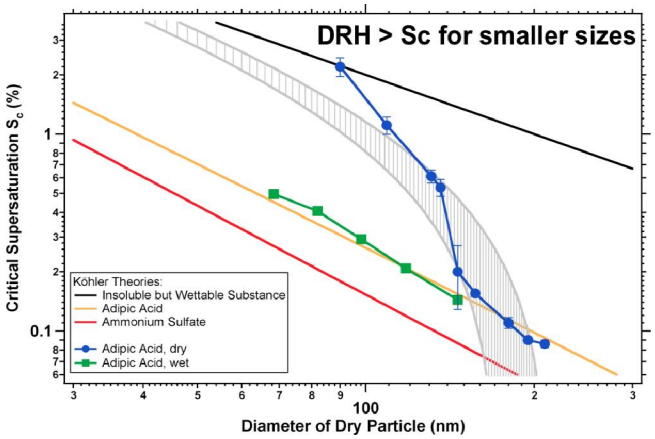

Figure 3. CCN activity of adipic acid particles under humid ('wet') and dry conditions; particle phase is very important for slightly soluble compounds.

2.3.2 Morphology Changes of Fractal Soot Particles Using Coating and Denuding Experiments: Implications for Optical Absorption and Atmospheric Lifetime. The morphology of soot particles was characterized by a series of studies as a function of coating and denuding. Low equivalence ratio laboratory flame soot (fractal-like) exhibits physical characteristics similar to diesel soot. Our experiments indicate that there is a regular relationship between the mobility diameter and mass of the soot particles (See Figure 4). Further, liquid and solid organic coatings do not significantly affect the underlying soot morphologies during coating and denuding experiments. In contrast, more recent work shows that inorganic (sulfuric acid) coatings collapse the soot structures.

Techniques were developed to measure the surface area of fractal soot particles. Experiments were conducted to measure particle mass, volume, density, composition, dynamic shape factor, fractal dimension, surface area, and the size and number of the primary spherules that form the fractal aggregate. By measuring these parameters before and after coating, it was shown that the surface area of fractal particles is up to 2.4 times greater than that of a sphere with the same d_m as the fractal particles. Using the surface area determinations, the atmospheric lifetime of a fractal particle was compared to lifetimes of spheres. If it is assumed (as it often is) that the fractal particle is a sphere with the same d_m as the fractal particle, the atmospheric lifetime is underestimated by a factor of up to 1.7. If the fractal particle is assumed to be a sphere with the same d_{ve} as the fractal particle, the magnitude of the underestimate is significantly larger. The work is described in *Slowik et al.* 2007b.

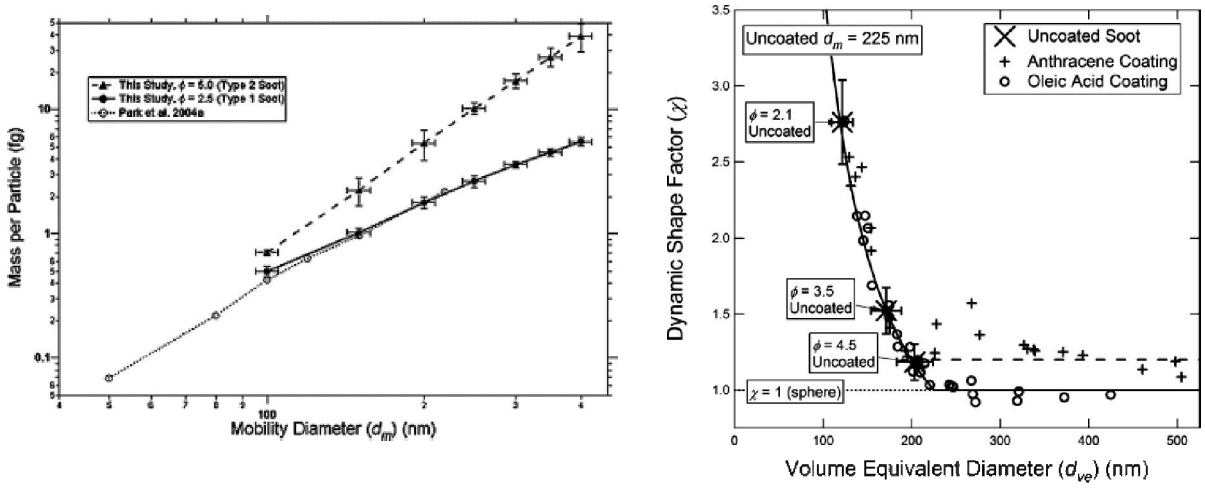

Figure 4. Results from the Boston College premixed laboratory flame experiments show behavior similar to diesel soot particles (left); particle shape affects size measurements and derived mass measurements. Coating soot particles with organic compounds (liquid oleic acid or solid anthracene) does not significantly affect soot physical properties (right).

2.3.3 Effect of Coatings on CCN activity of Soot Particles. Freshly generated soot particles do not exhibit CCN activity. An adipic acid coating on hydrophobic soot yields a CCN active particle, shown in Figure 5a. If the soot particle is relatively small ($d_{core} \leq 102$ nm), the CCN activity of the coated particles approaches the deliquescence line of adipic acid, suggesting that the total size of the particle determines CCN activation and the soot core acts as a scaffold.

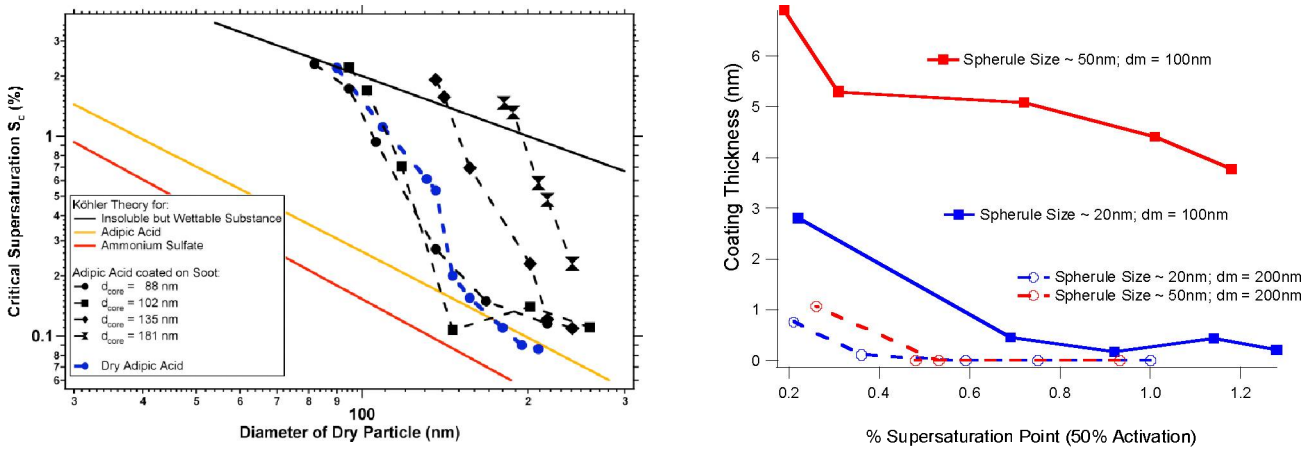

(refer to Figure 5).

Figure 5. (a) Adipic acid coated soot particles. (b) Thickness of sulfate coatings on fractal soot particles required to activate 50% of the particles. Particles of initial d_m = 100 nm (solid line) and 200 nm (broken line) were coated. The d_{pp} of the of the fractal aggregates composing the particles was either 20 nm (blue) or 50 nm (red).

(refer to Figure 5). However, as the soot particles become larger, the CCN activity is reduced, likely due to the inability of small amounts of adipic acid to fully coat the soot particles. A more detailed discussion is found in *Hings et al. 2008.*

In Figure 5b we show the effect of mobility diameter (d_m) and spherule diameter (d_{pp}) on CCN activity of ammonium sulfate coated fractal soot particles. The coating thickness is obtained by measuring particle d_m before and after coating. The coatings are applied onto particles of two initial mobility diameters, d_m = 100 nm and 200 nm. For each d_m, particles with two different spherule sizes were studied; d_{pp} = 20 nm and 50 nm. (Spherule size (d_{pp}) is determined by the flame temperature, set by the fuel-to-oxygen ratio.) The CCN activity of sulfate coated fractal soot particles increased with mobility diameter, but decreased with increasing spherule diameter. Again, exhibiting different CCN behavior based on the size and morphologies of the soot cores and the amount of the coatings. (See *Hings et al. 2008.*)

2.3.4 OH Oxidation of Combustion-related Particles. We performed extensive studies on the oxidation 'aging' of combustion related (soot and lubricating oil) and the effects of the oxidation on particle chemistry, morphology, and CCN activity. We studied the heterogeneous OH oxidation of soot aerosol particles as well as condensed phase organic aerosol particles composed of dioctyl phthalate (DOP). Both soot and DOP particles are initially CCN inactive.

The OH concentration was varied from 10 to 120 ppt. The oxidant exposure time was 240 seconds in all cases. Assuming a typical daytime atmospheric OH concentration of 0.1ppt, the laboratory experiments correspond to a continuous atmospheric exposure to OH varying from about 7 h to about 70 h. However, OH concentrations at the stated level of ~0.1 ppt are present only for about 6 hours out of the 24. Therefore, 240 s of exposure to OH at 120 ppt corresponds to about 12 days of atmospheric exposure to OH at 0.1 ppt. With some adjustments, about an order of magnitude higher concentration of OH was attained in subsequent experiments with our flow tube system.

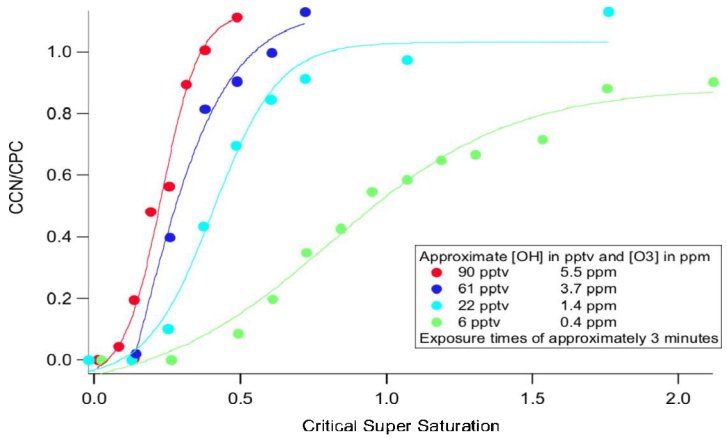

Figure 6. CCN activation data for flame-generated soot particles after varying exposures to gas-phase oxidant concentrations. Higher OH exposure increased CCN activity at lower supersaturations.

These experiments yielded some important results, a few of which are highlighted here. Figure 6 shows the CCN activity of flame-generated soot particles after exposure to varying amounts of oxidants in the flow tube. The CCN activity increases dramatically and systematically with OH concentration. The results shown in the figure indicate that at ~0.2% supersaturation, 163 nm soot particles will be fully activated after about a 9-day exposure to OH at atmospheric concentrations. (90 ppt for 240 s corresponds to about 9 days at 6 hrs/day and 0.1 ppt.) Similar results were obtained for the heterogeneous oxidation of DOP particle

These preliminary results showed that we can perform laboratory flow tube experiments on the oxidation of organic matter (gas phase and particulate) and measure subsequent changes in the resulting particles' CCN activity. The oxidant exposure levels achieved in the present flow tube arrangement are representative of aging in the atmosphere up to about 12 days. By increasing OH concentration and flow reactor residence times, atmospheric OH exposures of greater than two weeks has now been achieved. These multi-step oxidation methods are exhibiting chemical changes that mimic the observed O:C ratios in background ambient particles, a first for laboratory generated particles.

Relevance Coating and Oxidative Aging Studies of Soot Particles

The detailed characterization of chemical compositions, morphology, optical, and CCN properties of aged (coated and oxidized) combustion-related particles is required for modeling complete life-cycles and effects of combustion-related (e.g. soot) particles from anthropogenic, energy-producing sources. These studies are being extended under our current new DOE Award *No DE-SC0006980.*

3. Instrument Development and Characterization

3.1 Light Scattering Time-of-Flight Aerosol Mass Spectrometer (LS-ToF-AMS): At the center of our particle characterization instruments is the TOF-AMS developed by Aerodyne Research Inc. (ARI) with the participation of the Boston College research group. The instrument, shown schematically in Figure 7, is capable of rapidly measuring the ensemble average chemical composition and vacuum aerodynamic diameter size distribution (d_{va}) of sub-micron particles. When coupled with the light scattering module, the LS-ToF-AMS also provides the size and composition of single particles.

Particles are sampled from a gas flow at ambient pressure into an aerodynamic lens (2 torr). The lens has the dual purpose of focusing the particles into a narrow beam and, by the expansion of the gas into a vacuum (~10^{-4} torr), accelerating the particles to a velocity inversely related to their vacuum aerodynamic diameter (d_{va}). The particles strike a heated surface where the non-refractory components are vaporized. The resulting gas is ionized by electron impact (70 eV). The ions are detected with a calibrated time-of-flight mass spectrometer as shown in Fig. 7. The ToF-AMS provides the complete mass spectrum for each single particle event and can quantitatively measure single particle chemical composition for aerosol particles.

To extend the capability of the AMS as a stand-alone instrument, a light scattering module (LS) has been developed and incorporated into the AMS, as shown [*Cross et al. 2007*; *Cross et al., 2008*].

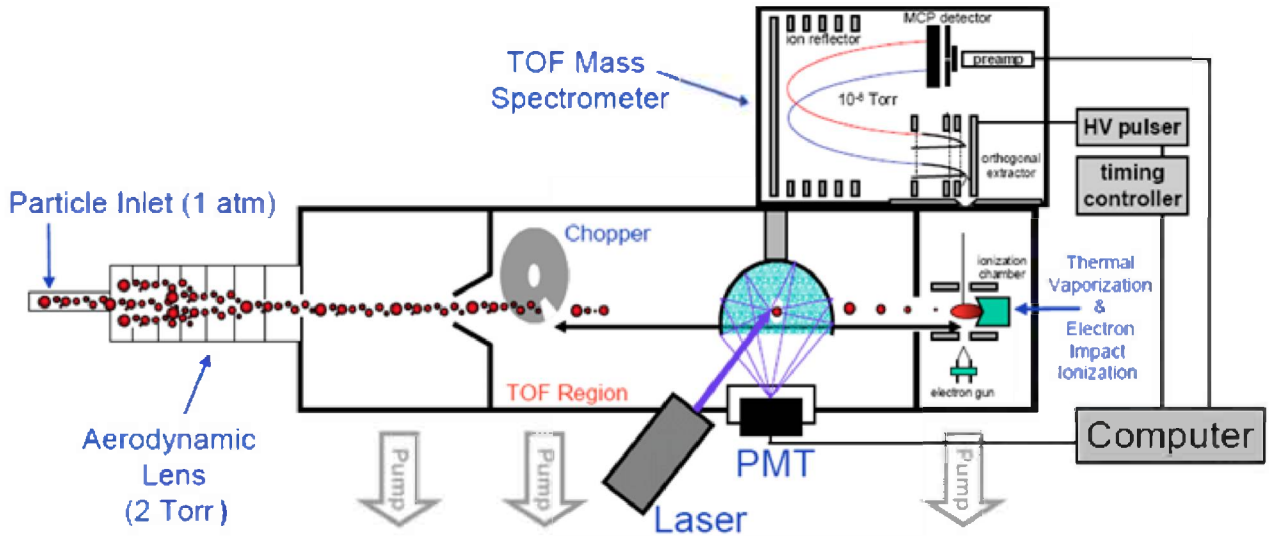

Figure 7. LS-TOF-AMS schematic

With the LS-TOF-AMS the magnitude of the scattered light signal (R_{LS}) and d_{va} are determined for every particle (refractory and non-refractory) with a size greater than the light scattering detection limit (~180 nm). By measuring the scattered light from a wide range of aerosol particles of known size, shape, and refractive index a single calibration curve, valid for atmospherically important aerosol particles, has been obtained. This calibration curve relates the magnitude of the scattered light signal (R_{LS}) to the optical diameter of the particles (d_o). The combination of the optical and aerodynamic diameters, allows one to calculate the particle density for spherical particles or effective density for non-spherical particles [*Cross et al. 2007*].

Our recent work has incorporated the LS module into the TOF-AMS systems which enable two very important applications: (1) the LS-TOF-AMS can operate as a true single particle instrument, and (2) the LS module allows for an internal measure of the collection efficiency of the system [Cross et al., 2008]. Sample results obtained during MILAGRO study in the summer of 2006 highlight the capabilities of the new system to determine the mixing state on a particle-by-particle basis in addition to measuring the standard ensemble averages of mass loading, chemistry, and size distributions [*Cross et al.*, 2006].

Knowledge of particle mixing in an aerosol ensemble is important in the evaluation of aerosol climate impacts. The ability to measure in real-time the single particle density and composition of ambient particles with the LS-TOF-AMS allowed the determination that the particles sampled at Chebogue Point, Nova Scotia during the Northeast Air Quality Study were internally mixed while in Mexico City during the MILAGRO study both internal and external mixtures were observed.

3.2 The Soot Particle Aerosol Mass Spectrometer (SP-AMS). The Soot Particle Aerosol Mass Spectrometer (SP-AMS) was developed to measure the chemical and physical properties of particles containing refractory black carbon. The instrument is a combination of two well-characterized instruments: The Aerodyne Aerosol Mass Spectrometer (AMS) and the Single Particle Soot Photometer (SP2) developed by Droplet Measurement Technologies. The SP-AMS is equipped with an intracavity laser vaporizer (1064 nm) in addition to the resistively heated, tungsten vaporizer used in a standard AMS. The data acquisition analysis tools are the same as for the standard AMS. The SP-AMS can be operated with the laser vaporizer alone, with both the laser and tungsten vaporizers, or with the tungsten vaporizer alone. When operating with only the laser vaporizer, the SP-AMS is selectively sensitive to laser-light absorbing particles, such as ambient refractory black carbon containing particles, and measures both the refractory and nonrefractory components. In this mode, other absorbing particles, such as metal nanoparticles, are also readily detected. When operated with both vaporizers and on and off laser modulation, the instrument measures both the refractory and total nonrefractory particulate matter.

Example results for the SP2AMS instrument are shown in Figure 8. These results show that the SP-AMS instrument is capable of measuring both the mass and size of black carbon containing particles. Specifically, the SP-AMS measurements include information on the chemical components of the coating and the core material. Currently, no other instrument can provide such detailed information in real time.

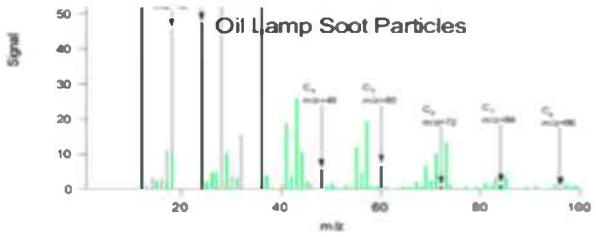

Figure 8. (a) Mass spectrum obtained by the SP-AMS instrument for oil lamp soot showing the black carbon ion clusters and organic coating material.

The SP-AMS instrument is currently being developed under a DOE Phase II project, and has been characterized in the Boston College laboratory utilizing the soot generation and conditioning equipment developed as part of the DOE ASP work. The SP-AMS mass spectral interpretation, calibration, and sensitivity are being studies and optimized under the sponsorship of our new DOE award No. DE-SC0006980. The utility of the instrument to characterize ambient refractory black carbon aerosol is being demonstrated.

3.3 Calibrating and characterizing the Photoelectric Aerosol Sensor (PAS, Echochem), the Single Particle Soot Photometer (SP2; DMT), photo-acoustic spectrometers (PAS; DRI and NOAA), and the Cavity-Assisted Phase-Shift (CAPS) extinction monitor (AR): In addition to instrument development, the Boston College and Aerodyne combined group is committed to calibrating and characterizing new instruments developed by other groups to measure important parameters, such as black carbon mass loadings and particle extinctions. In addition to the SP-AMS described above another instrument, designated as SP2 has been developed by DMT. This instrument measures black carbon mass loadings based on incandescence techniques. The instrument has been extensively characterized in the Boston College laboratory with our soot aerosol generation and conditioning equipment. Furthermore, our laboratory has been used to calibrate and characterize the responses of the Ecochem PAS instrument to nascent and coated soot particles and newly developed photoacoustic (DRI and NOAA) and CAPS-based extinction instruments (ARI). This work is in addition to the two extensive laboratory inter-comparison projects we have hosted as part of the DOE ASP project (described below in Section 5). Results from our study on the PAS (Ecochem) instrument were included in the analysis of Polycyclic Aromatic Hydrocarons (PAH) emissions during MCMA2003 study [*Marr et al., 2006*]. Recent results from these studies are being incorporated into manuscripts under preparation.

4. Field Studies.

During the period covered in this report, our Boston College/ Aerodyne group participated in two field studies; the Northeast Air Quality Study (NEAQS) in the summer of 2004 and the Mexico City Metropolitan Area (MCMA) study as part of the MILAGRO field study, in March of 2006. (The MILAGRO study and the data analysis of the NEAQS study were conducted during the past funding period.) The NEAQS study demonstrated the ability of the AMS instrument equipped with the light scattering module to measure the density of ambient aerosol particles (*Cross et al. 2007*). The results of the MILAGRO study were more extensive (*Cross et al. 2008*).

An Aerodyne time-of-flight aerosol mass spectrometer coupled with a light scattering module was deployed at the T1 ground site approximately 40 km northeast of the Mexico City Metropolitan Area (MCMA) as part of the MILAGRO field study in March of 2006. Over a 74 hour sampling period 12,853 single particle mass spectra were optically triggered and saved. In addition to the single particle data, the instrument also acquired average chemical composition and average vacuum aerodynamic diameter size distributions for the ambient aerosol particle ensemble.

The following results were obtained: Using the single particle detection capabilities of this instrument, the detection efficiency of the AMS was quantitatively determined. The single particle mass measurement was shown to be in quantitative agreement with average ensemble mass measurements. The single particle mass components were categorized into HOA, OOA, NH_4NO_3, $(NH_4)_2SO_4$, and NH_4Cl fractions and were displayed as a function of sampling time. The measurement of chemical composition allowed the identification of time periods during which the ambient ensemble was externally mixed. In some cases the chemical composition of the particles suggested a likely source. During morning rush hour (04:00-09:00 AM) each day the ambient ensemble was an external mixture of combustion-generated HOA particles from local traffic and regionally-influenced particles of mixed composition. From 09:00-11:00 AM

all particles within the ambient ensemble become coated with NH_4NO_3 mostly likely due to photochemical production HNO_3. In one instance, gas-to-particle condensation of $(NH_4)_2SO_4$ is observed within a strong SO_2 (g) plume arriving at T1 from the northwest. Particles with high NH_4Cl mass fractions were identified during early morning periods. Particles with mass spectral features characterized by biomass burning were also identified (*Cross et al. 2008*).

To illustrate the physical and chemical information obtained with the LS-ToF-AMS, we examine a case when two particles entered the AMS during one chopper opening, recorded at 5:35 LT on March 27th – during the morning rush hour. (Under the ambient particle concentrations observed during the experiment, we expect such a two-particle coincidence to occur ~ 1% of the time.) The top panel of Figure 9 shows the scattered light pulses from the two particles as a function of time-of-flight, with t_0 defined by the opening of the chopper slit. The middle panel shows the corresponding chemical ion signals. The lower panel displays the mass spectrum for each of the sampled particles.

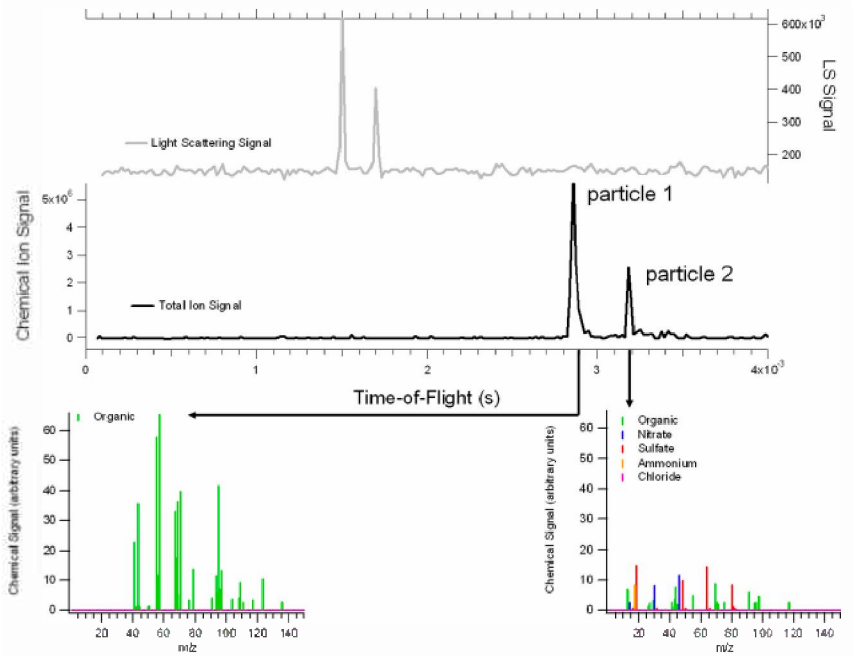

Figure 9. Light scattering signals (upper panel) and chemical ion signals (middle panel) as a function of particle time-of-flight for a single chopper cycle in which two particles entered the LS-ToF-AMS. The lower panel displays the mass spectrum of each particle.

The separation in particle time-of-flight indicated different particle effective densities and the single particle mass spectra in bottom of Figure 8 clearly show that the chemical compositions of the two sampled particles are distinct. Particle 1 is composed of 100% organic material. The largest mass spectrum component is at m/z = 57 characteristic of an HOA particle. Particle 2 is a mixture of oxygenated organics, ammonium nitrate, and ammonium sulfate approximately in equal amounts. The observation of two distinct particle types within the same

chopper cycle indicates that the ambient ensemble was externally mixed during this sampling period.

Combining the chemical and physical information collected by the LS-ToF-AMS from these two particles tells a self-consistent story. Particle 1 was composed of hydrocarbon-like organic matter and exhibited a low effective density. The low effective particle density is consistent with hydrocarbon-like organic (e.g. lubricating oil) densities as well as possibly indicating that Particle 1 was non-spherical due to an underlying fractal-like black carbon core. Thus, particle 1 can be identified as a pure HOA particle likely generated from a local combustion source. In contrast, Particle 2 was composed of highly oxidized inorganic and organic matter and exhibited a relatively high effective density consistent with the particle's significant inorganic composition. Particle 2 was an internally mixed accumulation mode particle that likely had undergone significant atmospheric processing prior to detection with the LS-ToF-AMS. The simultaneous observation of these two externally mixed particles illustrates the capabilities of the LS-ToF-AMS technique to provide a measure of the mixing state and atmospheric processing of ambient submicron aerosol particles.

Figure 10 highlights the mixing state information obtained from the LS-TOF-AMS during MILAGRO study. Figure 10a shows the total number of externally mixed HOA particles detected as a function of the time of day (local time) and the ratio of the uncoated to coated HOA particles.

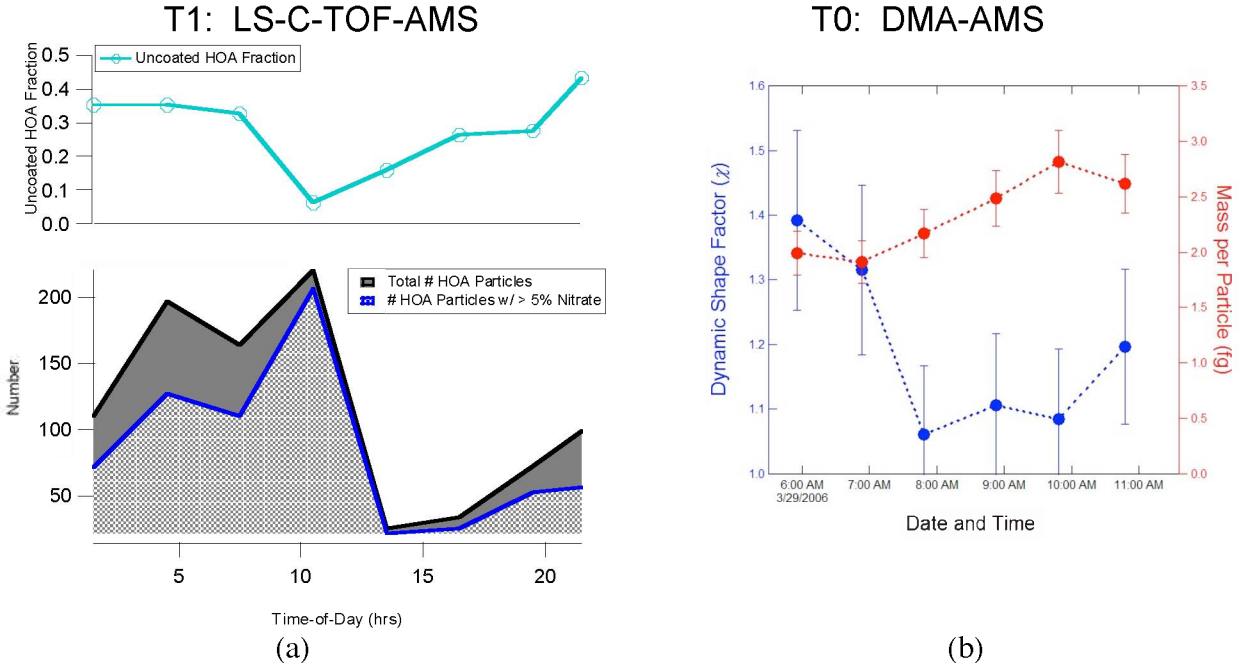

Figure 10. (a) LS-TOF-AMS single particle information from T1 site during MILAGRO showing the processing of externally mixed HOA. (b) SMPS-AMS observations obtained at T0 showing the changes in morphology and mass of soot particles during the same time periods.

The dramatic dip during the morning before 10AM is a direct measure of the photo-oxidation occurring that rapidly coats all of the observed HOA particles with secondary organic

and inorganic gas-to-particle compounds. Observations obtained at T0 using a combined SMPS-AMS instrument, shown in Figure 10b, obtained similar results. Both measurements provide important insights into the speed and magnitude of the atmospheric processing that occurs on emitted, primary combustion-related particles in Mexico City.

5. Inter-Comparison of Instruments Measuring Black Carbon Content of Soot Particles.

In recent years multiple techniques have been developed for measuring, in real-time, the black carbon (BC) content of particles. Such methods are based either on the unique thermal properties of BC or its optical properties. However, to actualize this potential, these instruments, based on very different approaches, have to be calibrated, and their performances have to be validated. The Boston College - Aerodyne soot particle generation and conditioning equipment (Figure 1) and aerosol characterization equipment based on AMS technologies are capable of providing real-time, well-characterized soot particles for such instrument inter-comparisons.

An indispensable step in the testing and validation of BC measuring instruments are inter-comparison studies that under controlled conditions, calibrate and compare results provided by different instruments designed to measure the same or related parameters. Such inter-comparison measurements are necessary if one is to reduce the large uncertainties associated with aerosol effects on climate.

5.1 The First Inter-comparison Study. In May 2005 the first inter-comparison study was conducted at the Boston College laboratories to measure the BC mass of well-characterized soot particles produced by a combustion source developed by the Boston College-Aerodyne research group (*Slowik et al., 2007*). Response to black carbon in soot particles of the following four instruments was inter-compared under a range of experimental conditions: the Aerosol Mass Spectrometer-Scanning Mobility Particle Sizer (AMS-SMPS) (*Slowik et al., 2004*; *DeCarlo et al. 2004*), the Single Particle Soot Photometer (SP2), the Multi-Angle Absorption Photometer (MAAP), and the Photoacoustic Spectrometer (PAS). These instruments provided measurements of the refractory mass (AMS-SMPS), incandescent mass (SP2) and optically-absorbing mass (MAAP and PAS). An optical detection module in the AMS and a Scanning Electron Microscopy (SEM) sampling system were also employed [*Chakrabarty et al., 2007, 2008*, and *2009*]. The results from this intitial instrument intercomparison are summarized in *Slowik et al., 2007a.*

Perhaps the most important contribution from the initial study was the successful, first calibration of the SP2 instrument as a function of true black carbon particle mass, shown in Figure 11. This calibration was used directly in subsequent SP2 studies and has provided the confidence within the atmospheric aerosol community to apply the SP2 instrument as a real-time, single particle black carbon instrument to many important, subsequent field studies [*Schwarz et al., 2006; Gao et al., 2007*].

5.2 The Second Inter-comparison Study. A follow on inter-comparison study was conducted in July 2008 featuring an improved soot particle source and including a wider array of black carbon instrumentation.

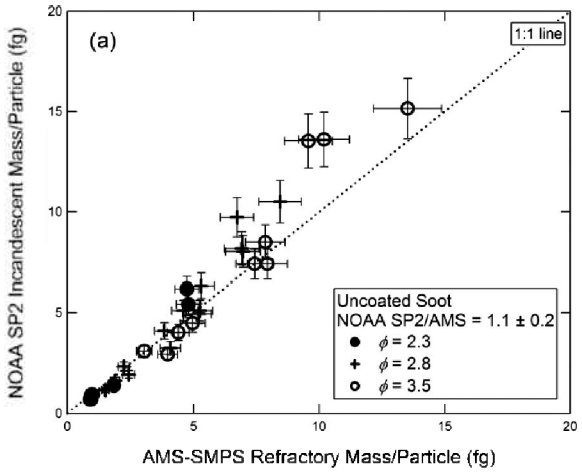

Figure 11. Calibration of the incandesnce signal of the SP2 instrument as a function of the black carbon content of uncoated soot particles for three flame equivalence ratio.

The new re-designed source has greatly improved stability and provides monodisperse, size selected soot particles in an extended d_m range 30 nm to 300 nm. The particle size distribution is narrower and more clearly defined. The particles are more accurately characterized with respect to mobility diameter, aerodynamic diameter, composition, fractal dimension and shape factor. The fuel-to-oxygen ratio and particle concentrations are all more accurately controlled and measured. In the first inter-comparison study, the particle flow rate was limited to about ~ 3 L/min. Re-configuration of the flow system, allowed simultaneous measurement of soot particles with as many as 18 instruments requiring total flow of ~ 22 L/min. (This includes monitoring instruments to characterize the flow.) Stable adjustable control of relative humidity in the particle carrier gas is another new feature of the re-designed system.

The performances of 19 instruments were inter-compared in the 2008 study. Of these instruments 9 were mass-based and 8 were optical-based. Each instrument provided real-time or near real-time measurements. Samples were also collected for subsequent electron microscope imaging and thermal optical analysis. Twenty-seven people representing 12 institutions from governmental laboratories, academia and industry participated in the project. The projects science goals, participating instruments, participating institutions, and individual participants are described in Cross et al. 2010.

In the course of three weeks, 318 runs were performed covering a matrix that systematically tested the performance of each instrument over a range of relevant parameters. Opportunity was provided for each instrument to sample soot particles as a function of the following controlled and measured (directly or indirectly) parameters: particle mobility size ($30 \leq d_m \leq 300$ nm), particle number concentration (500-50,000 p/cc), particle shape (dynamic shape factor and fractal dimension), particle chemistry and density (changed via coatings), black carbon mass, and relative humidity (5-90%). In the selected runs with coated particles, the coating thickness of H_2SO_4 or DOS was measured via the change in mobility diameter (Δd_m) in the range ($1 \text{ nm} \leq \Delta d_m \leq 150$ nm). In addition to flame-generated soot, black carbon particles

were also obtained by atomizing fullerene soot, glassy carbon spheres, oxidized flame soot, Regal black toner, and Aquadag paint.

The following instruments were tested: Aerosol Mass Spectrometer-Scanning Mobility Particle Sizer (AMS-SMPS) combination, Single Particle Soot Photometer (SP2), and Photoacoustic Spectrometer (PAS). These instruments provided measurements of the refractory mass (AMS-SMPS), a Soot Particle Aerosol Mass Spectrometer (SP-AMS), a Couette Centrifugal Particle Mass Analyzer (CPMA), a Photo-acoustic Soot Spectrometer (PASS-3), a Photo-Thermal Interferometer (PTI), a Cavity-Ring Down (CRD) Extinction Spectrometer, a Cavity Attenuated Phase Shift (CAPS) Extinction Monitor, and a Nephelometer.

6. Data processing and Analysis of Results of Experiments Inter-Comparing Instruments Measuring Black Carbon Content of Soot Particles. For purposes of discussion we divide the instruments in this study into two categories; mass based and optically based. Mass based instruments measure parameters that are directly or computationally related to BC mass. Here empirical inter-comparison of mass-based instruments utilizing different principles validates instrument calibration and performance.

The optically based instruments measure absorption and/or scattering by particles containing black carbon including particles with known coatings. Calibration with well-characterized particles empirically connects the absorption and scattering measurements with the properties of the particles.

The following tasks were accomplished:

6.1. Experimental Objectives and Selected Results for Mass-Based Instruments.

a) Couette Centrifugal Particle Mass Analyzer (CPMA). In conjunction with the SMPS and the CPC instruments, the CPMA provides the most direct shape indendent measure of absolute particle mass. The purpose of this part of the study was to (**a**) validate the calibration of the CPMA instrument, (**b**) measure the black carbon mass content of soot particles and (**c**) measurement the fractal dimension of soot particles.

These tasks were accomplished. In addition it was shown that both the H_2SO_4 and BES coatings make the fractal soot particles more spherical in shape increasing the fractal dimension from D_f ~ 2.2 to 2.88 and 3.06 for H_2SO_4 and BES respectively. After denuding, the particles that had been coated with BES returned (within experimental accuracy) to their original soot particle fractality. On the other hand, the H_2SO_4 coated soot particles after denuding are found to be significanly more spherical than the nascent soot particles. This coating-denuding effect is displayed clearly in electron micrographs. It appears that a liquid coating brings about a colaps of the soot fractal structure. But the BES coating that is a solid at room temperature does not alter the underlying soot structure.

b) Comparison of CPMA and AMS-SMPS Instruments. Both the CPMA and AMS-SMPS instruments provide a particle mass determination. There is however an important difference between the data provided by the two instruments. The CPMA yields the total per particle mass and does not provide a separate evaluation of the black carbon mass in the particle. The AMS-SMPS instrument measures directly only the non-refractory particle mass. It does however provide a measure of the refractory (i.e. black carbon) mass in the same particle but indirectly, via a fitting procedure involving black carbon mass, volume equivalent diameter (d_{ve}) and the

dynamic shape factor (defined as the ratio of the drag on a particle to the drag on a sphere with diameter d_{ve}). The objective of the experiments described in this section is to inter-compare these two instruments that measure particle mass in different ways. The agreement between the two independent total particle mass measurements provides a validation of the black carbon determination by the AMS-SMPS instrument.

c) Performance Study of the SP2 Instruments. Three Soot Particle Soot Photometer (SP2) instruments were tested in these studies. The instruments are owned respectively by University of Hawaii (UH), Droplet Measurement Technologies (DMT) and NOAA CIRES. The experiments with the SP2 instruments had the following goals: **(a)** Measure, inter-compare and calibrate the incandescence signals obtained from the three SP2 instruments as a function of black carbon particle mass. **(b)** Investigate how BES and H_2SO_4 coatings affect the SP2 measurements. **(c)** Determine the effect of particle shape the SP2 measurements and **(d)** Determine the lower limit on d_m for accurate measurement of BC mass in soot particles. These goals were successfully accomplished.

6.2. Experimental Objectives and Selected Results for Optical Absorption and Extinction Based Instruments. Both optical absorption based and extinction based instruments were tested in the present studies. The absorption-based instruments studied were: Photoacoustic Spectrometer (PAS), Photoacoustic Soot Spectrometer (PASS-3), and Photo-thermal Interferometer (PTI). The PAS and PTI instruments measure absorption at *wave length* = 532 nm. The PASS-3 measures absorption at three wavelengths, *wave length* = 405 nm, 532 nm, and 781 nm.

The extinction based instruments studied were: Cavity Ring Down Aerosol Extinction Spectrometer (CRD-AES) and Cavity Attenuated Phase Shift Extinction Monitor (CAPS). The CRD-AES instrument operates at three wavelengths, λ = 355 nm, 532 nm, and 1064 nm. The CAPS instrument operates at *wave length* = 440 nm. The experiments with these instruments had goals similar to those for the mass based instruments. The following were the goals and the tasks accomplished:

(a) Measure, inter-compare and calibrate the mass specific absorption or extinction cross sections provided by the instruments as a function of black carbon particle mass. The mass specific absorption cross sections were measured at 532 nm by the PAS and PTI instruments and at 405 nm, 532 nm, and 781 nm by the PASS instrument. From this data the mass specific absorption coefficient was obtained.

(b) Investigate the effect of coatings (coating present on nascent soot, BES and H_2SO_4 coatings) on the measurements of mass specific absorption or extinction cross sections. The effect of BES and H_2SO_4 coatings on the measurements provided by the PAS, PASS and PTI was measured.

(c) Determine the effect of particle shape on measurements. As was stated, H_2SO_4 coated soot particles after denuding are found to be significanly more spherical than the nascent soot particles. The effect of shape change on the mass specific absorption coefficient was determined.

(d) Determine the lower limit on d_m for accurate measurement of mass specific absorption and extinction cross sections for soot particles. The lower limit on d_m for accurate measurement of

mass specific absorption cross section were determined. A similar set of data was obtained for the CRD-AES, and CAPs extinction based instruments over the range 355 nm to 1064 nm.

- A manuscript providing an overview of the inter-comparison studies and more detailed description of results has been published (*Cross et al. 2010*)

Over the past three years the operating range for instrumentation has been extended and a number new instruments have been developed. Once again an inter-comparison of instruments is needed. *We are planning such an inter-comparison study to be held during the summer of 2012 sponsored by our new DOE award No DE-SC0006980. Sixteen research groups have expressed a strong interest in participating.*

7. Absorption Enhancement of Coated Absorbing Aerosols: Validation of the Photo-Acoustic Technique for Measuring the Enhancement. In a collaborative project with Daniel A. Lack and Paola Massoli (both at NOAA Earth System Research Laboratory and UC Boulder), and Chris D. Cappa (U C Davis) we conducted a series of experiments to measure absorption enhancement of coated absorbing aerosols and thereby validate the photo-acoustic technique for measuring the enhancement. A cavity ring down aerosol extinction spectrometer (CRD-AES) and a photo-acoustic absorption spectrometer (PAS) were used, in conjunction with Mie Theory, to measure the refractive index (RI) of absorbing polystyrene spheres (APSS). The CRD-AES and PAS were also used to measure the extinction and absorption enhancement after these APSS were coated in oleic acid. The experimental enhancements were then compared to predictions from two-layer Mie Theory. The measured extinction and absorption enhancements both agreed with modeled enhancements to within an average of 5 percent. A filter-based absorption technique was also used to measure the absorption by the APSS and showed a significant size-dependant bias, as evidenced by the filter-based method measuring significantly lower absorption for both un-coated and coated APSS compared to the PAS. These results suggest the validity of applying photo-acoustics to measure the absorption enhancement created by semi-volatile atmospheric species coating absorbing particles. This work has now been published in *Lack et al. 2009.*

8. Characterization of Aerosol Photooxidation Flow Reactors: Heterogeneous Oxidation, Secondary Organic Aerosol Formation, and Cloud Condensation Nuclei Activity Measurements. Motivated by the need to develop instrumental techniques for characterizing organic aerosol aging, we report on the performance of the Toronto Photo-Oxidation Tube (TPOT) and Potential Aerosol Mass (PAM) flow tube reactors under a variety of experimental conditions. The principal difference between the flow tubes was that the PAM system was designed to minimize wall effects, whereas the TPOT reactor was designed to study heterogeneous aerosol chemistry. The following studies were performed: (1) transmission efficiency measurements for CO_2, SO_2 and bis(2ethylhexyl) sebacate (BES) particles, (2) H_2SO_4 yield measurements from the oxidation of SO2, (3) residence time distribution (RTD) measurements for CO_2, SO_2, and BES particles, (4) chemical composition and cloud condensation nuclei (CCN) activity measurements of BES particles exposed to OH radicals, and (5) chemical composition, CCN activity, and yield measurements of secondary organic aerosol (SOA) generated from gas-phase OH oxidation of m xylene and a pinene. OH exposures ranged from (2.0) 10^{10} to (1.8) 10^{12} molec cm^{-3} s. Where applicable, data from the flow tube reactors are

compared with published results from the Caltech smog chamber. The TPOT yielded narrower RTDs. However, its transmission efficiency for SO_2 was lower than that for the PAM. Transmission efficiency for BES and H_2SO_4 particles was size-dependent and was similar for the two flow tube designs. Oxidized BES particles had similar chemical composition and CCN activity at OH exposures greater than 10E(11) molec cm^{-3} s, but different CCN activity at lower OH exposures. The composition and yield of m xylene and a pinene SOA was strongly affected by reactor design and operating conditions, with wall interactions seemingly having the strongest influence on SOA yield. At comparable OH exposures, flow tube SOA was more oxidized than smog chamber SOA because of faster gas-phase oxidation relative to particle nucleation. SOA yields were lower in the TPOT than in the PAM, but CCN activity of flow-tube-generated SOA particles was similar. For comparable OH exposures, a-pinene SOA yields were similar in the PAM and Caltech chambers, but m-xylene SOA yields were much lower in the PAM compared to the Caltech chamber. (*Lambe et al., 2011*)

9. Relationship between aerosol oxidation level and hygroscopic properties of laboratory generated secondary organic aerosols (SOA). Laboratory experiments are currently conducted to investigate the relationship between degree of oxidation and hygroscopic properties of secondary organic aerosols (SOA). We generate SOA from a range of precursors among them a-pinene, 1,3,5 trimethylbenzene (TMB) and m-xylene SOA (proxies for both biogenic and anthropogenic SOA systems) via OH oxidation of gaseous precursors in an aerosol flow reactor. The degree of aerosol oxidation is represented by the atomic O/C ratio, as measured by the Aerodyne High Resolution Time of Flight Aerosol Mass Spectrometer (HR ToF). A Hygroscopicity Tandem Differential Mobility Analyzer (HTDMA) measures the hygroscopic growth factor (HGF). A CCN instrument directly measured the aerosol CCN activity, here expressed by the single parameter κ. This work is now being conducted under our new DOE Award No. DE-SC0006980 and will be described in upcoming publications and reports.

REFERENCES

Only references directly describing the work in this report are provided.

- **The publications associated with the DOE sponsored research Award Register#: ER639950011068 are marked with an asterisk.**

*Canagaratna, M. R., J. T. Jayne, J. L. Jiménez, J. D. Allan, M. R. Alfarra, Q. Zhang, T. B. Onasch, F. Drewnick, H. Coe, A. Middlebrook, A. Delia, L. R. Williams, A. M. Trimborn, M. J. Northway, P. F. DeCarlo, C. E. Kolb, P. Davidovits, and D. R. Worsnop, "Chemical and Microphysical Characterization of Ambient Aerosols with the Aerodyne Aerosol Mass Spectrometer", *Mass Spectrometry Reviews*, *26*, 185-222, 2007.

*Chakrabarty, R.K., H. Moosmüller, W. P. Arnott, M. A. Garro, J. G. Slowik, E. S. Cross, J.-H. Han, P. Davidovits, T. B. Onasch and D. R. Worsnop, "Light Scattering and Absorption by Fractal-Like Carbonaceous Chain Aggregates: Comparison of Theories and Experiment," *Applied Optics*, Vol. 46, 28, 2007, pp. 6990-7006, 2007.

*Chakrabarty, R.K., H. Moosmüller, M. A. Garro, W. Patrick Arnott, J. G. Slowik, E. S. Cross, J. H. Han, P. Davidovits, T. B. Onasch and D. R. Worsnop, "Morphology based particle

segregation by electrostatic charge," *Journal of Aerosol Science*, Vol. 39, 9, pp. 785-792, 2008,

*Chakrabarty, R.K., H. Moosmüller, W. P. Arnott, M. A. Garro, G. Tian, J. G. Slowik, E. S. Cross, J.-H. Han, P. Davidovits, T. B. Onasch and D. R. Worsnop, "Low fractal dimension cluster-dilute soot aggregates from a premixed flame," *Physical Review Letters*, 102, 235504, DOI: 101103/PhysRevLett. 102.235504, July 12, 2009.

*Cross, E. S., J. G. Slowik, P. Davidovits, J. D. Allan, D. R. Worsnop, J. T. Jayne, D. K. Lewis[+], M. Canagranata, and T.y B. Onasch, Laboratory and Ambient Particle Density Determinations using Light Scattering in Conjunction with Aerosol Mass Spectrometry, *Aerosol Sci. Tech.*, *41*, 343-359, 2007.

*Cross, E. S., T. B. Onasch, M. R. Canagaratna, J. T. Jayne, J. R. Kimmel, X. Y. Yu, M. L. Alexander, D. R. Worsnop, and P. Davidovits, Single particle characterization using a light scattering module coupled to a time-of flight aerosol mass spectrometer, Atmos. Chem. Phys. Discuss., 8, 21313-21381, 2008.

DeCarlo, P.F., J. G. Slowik, D. R. Worsnop, P. Davidovits and J. L. Jimenez, "Particle Morphology and Density Characterization by Combined Mobility and Aerodynamic Diameter Measurements. Part 1: Theory," Aerosol Science and Technology, Vol. 38, pp. 1185–1205, 2004.

*Gao, R. S., J. P. Schwarz, K. K. Kelly, D. W. Fahey, L. A. Watts, T. L. Thompson, J. R. Spackman, J. G. Slowik, E. S. Cross, J.-H. Han, P. Davidovits, T. B. Onasch and D. R. Worsnop, "A Novel Method for Estimating Light-Scattering Properties of Soot Aerosols Using a Modified Single-Particle Soot Photometer," *Aerosol Science and Technology*, Vol. 41, pp. 125-135, 2007.

*Lack, D. A. Chris D. Cappa, Eben S. Cross, Paola Massoli, Adam T. Ahern, Paul Davidovits and Timothy B. Onasch. "Absorption Enhancement of Coated Absorbing Aerosols: Validation of the Photo-Acoustic Technique for Measuring the Enhancement" Aerosol Science and Technology, 43, 10006-1012, DOI: 10.1080/0278682093117932, October 2009.

*Hings, S. S., W. C. Wrobel, E. S. Cross, D. R. Worsnop, P. Davidovits, and T. B. Onasch, "CCN Activation Experiments with Adipic Acid: Effect of Particle Phase and Adipic Acid Coatings on Soluble and Insoluble Particles", *Atmospheric Chemistry and Physics Discussions*, *8*, 4439-4482, 2008.

Jayne, J. T., D. C. Leard, X. Zhang, P. Davidovits, K. A. Smith, C. E. Kolb, and D. R. Worsnop, Development of an Aerosol Mass Spectrometer for Size and Composition Analysis of Submicron Particles, *Aerosol Sci. Technol.*, *33*, 49-70, 2000.

*Marr, L. C., K. Dzepina, J. L. Jimenez, F. Reisen, H. L. Bethel, J. Arey, J. S. Gaffney, N. A. Marley, L. T. Molina and M. J. Molina, "Sources and transformations of particle-bound polycyclic aromatic hydrocarbons in Mexico City," *Atmos. Chem. Phys.*, Vol. 6, pp. 1733–1745, 2006.

*Schwarz, J. P., et al., Single-particle measurements of midlatitude black carbon and light-scattering aerosols from the boundary layer to the lower stratosphere, J. Geophys. Res., 111, D16207, doi:10.1029/2006JD007076, 2006.

Slowik, J.G., K. Stainken, P. Davidovits, L.R. Williams, J.T. Jayne, C.E. Kolb, and D.R. Worsnop,Y. Rudich P. DeCarlo, J.L. Jimenez (2004), Particle Morphology and Density Characterization by Combined Mobility and Aerodynamic Diameter Measurements. Part 2:

Application to Combustion Generated Soot Aerosols as a Function of Fuel Equivalence Ratio, *Aerosol Sci. Tech.*, *38*, 1206-1222, 2004.

*Slowik, J. G., E. S. Cross, J-H. Han, P. Davidovits, T. B. Onasch, J. T. Jayne, L. R. Williams, M. R. Canagaratna, D. R. Worsnop, R. K. Chakrabarty, W. P. Arnott, J. P. Schwarz, R-S. Gao, D. W. Fahey, G. L. Kok, D. G. Baumgardner, An Inter-Comparison of Instruments Measuring Black Carbon Content of Soot Particles, *Aerosol Sci. Tech.*, *49*, 295-314, 2007a.

*Slowik, J.G., E. S. Cross, J-H. Han, J. Kolucki, P. Davidovits, L. R. Williams, T. B. Onasch, J. T. Jayne, C. E. Kolb, D. R. Worsnop, Measurements of Morphology Changes of Fractal Soot Particles using Coating and Denuding Experiments: Implications for Optical Absorption and Atmospheric Lifetime, *Aerosol Sci. Technol.*, *41* (8), 734 – 750, DOI: 10.1080/02786820701432632, 2007b.